Materials Research Proceedings **26** (2023) 195-200 https://doi.org/10.21741/9781644902431-32

A novel prototype of diaphragm valve for passively compensated aerostatic pads

Federico Colombo [1, a], Luigi Lentini [1,b*], Terenziano Raparelli[1,c], Andrea Trivella[,4c]

[1]Politecnico di Torino, Corso Duca degli Abruzzi 24, 10129, Turin, Italy

afederico.colombo@polito.it , bluigi.lentini@polito.it , cterenziano.raparelli@polito.it , dandrea.trivella@polito.it

*corresponding author

Keywords: Air Pad, Gas Bearings, Infinite Stiffness, Compensation, Diaphragm Valve

Abstract. Thanks to their low friction, aerostatic pads are currently used in many high precision applications. However, due to the air compressibility, aerostatic bearings suffer from relatively low stiffness and damping. Active and passive compensation methods represent a valuable solution to reduce these limitations. This paper presents a novel prototype of a diaphragm valve for passively compensated aerostatic pads. The proposed valve was obtained through the improvements of a previous prototype. The main goal of this new design of the valve was to improve the reliability, repeatability and accuracy of regulation. The novel prototype is modelled through the same lumped parameter model that was used for the previous prototype. The preliminary experimental results demonstrate the efficiency and effectiveness of the proposed valve.

Introduction

Because their zero friction, aerostatic pads are widely used in applications where high precision of positioning is required, e.g., machine tools and measuring machines [1,2]. However, this kind of bearings are characterized by low relative stiffness and they suffer from low damping due to the air compressibility. In this regard, different solutions have been proposed to improve aerostatic pad performance. In the attempt of reducing these limitations different kinds of feeding system were studied and experimented, e.g., multiples supply holes with different size, number and location [3], porous inserts or surfaces [4,5] and compound restrictors [6–8]. However, a suitable choice and design of the feeding system of aerostatic pads can lead only to limited performance improvement. Conversely, active and passive compensation methods make it possible to significantly improve both static and dynamic performance [9,10]. Passive compensation methods use components which require only the energy associated with the supply pressure of the bearing, e.g., pneumatic valves and compliant elements. By contrast, actively compensated bearings exploit elements that require external sources of energy to function, e.g., sensors, controllers and actuators. Although their high performance [11–13], active compensation solutions are still too expensive and thus result to be unsuitable for industrial applications. Notwithstanding their lower bandwidth, passive compensation solutions represent a cheaper alternative. This paper presents a novel prototype of passively compensated pad. This passive compensation solution consists in the integration of commercial pad and a custom-built diaphragm valve whose design is an improved version of that described in [14,15]. The novel prototype is modelled through the same lumped parameter model that was used for the previous prototype.

Materials Research Proceedings **26** (2023) 195-200 https://doi.org/10.21741/9781644902431-32

The Prototype

Figure 1a and 1b show a cross section of the designed diaphragm valve and the aerostatic pad.

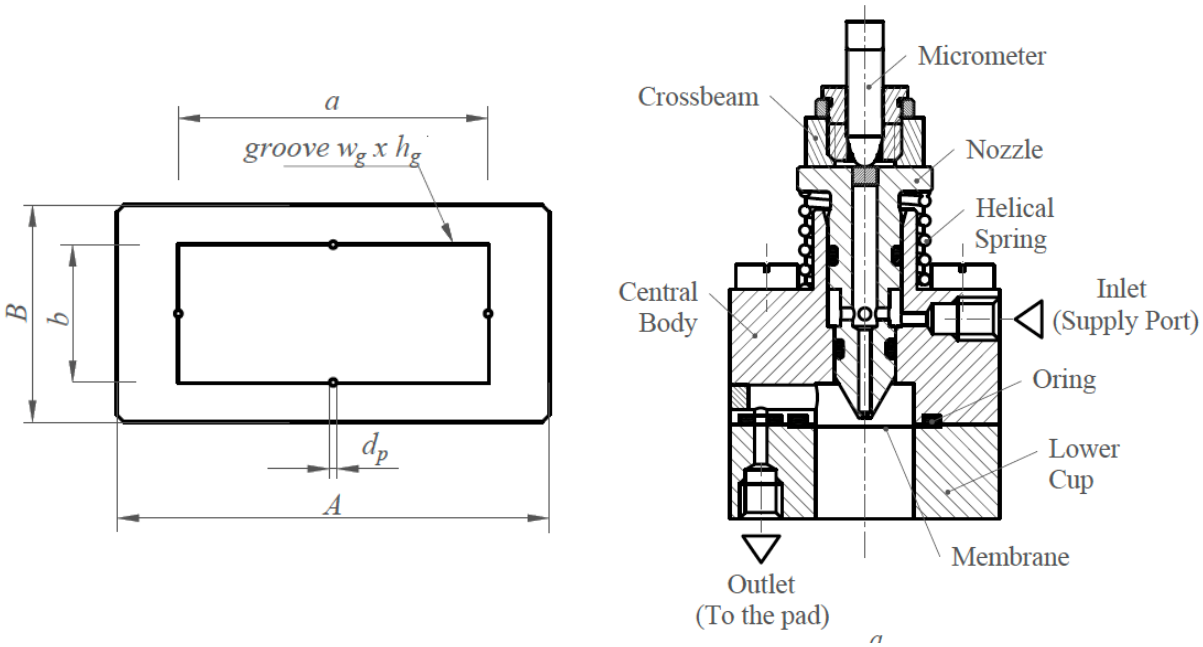

(a) Air pad. (b) Diaphragm valve.

Figure 1: The proposed prototype.

The diaphragm valve is composed of three main parts: an upper crossbeam, a central body and a lower cap. The chamber of the valve is located at the interface between the central body and the lower cap. The lower surface of the chamber consists of a membrane that is clamped between the central body and the lower cup thanks to the presence of an elastomeric o-ring. The chamber of the valve is supplied through a moving nozzle. The relative position from the nozzle and the membrane can be manually regulated through a micrometer. A coil spring is compressed between the nozzle and the central body to guarantee the presence of a restoring force when the nozzle must be moved upwards. The main goal of the novel design was to modify the mechanism to regulate the initial nozzle-membrane distance, i.e., when the system is not pressurized, since the accuracy, repeatability and reliability of the system is strictly related to this aspect. The air pad has rectangular base of 60x30 mm^2 (AxB) and four orifices with a diameter of 1 mm (d_p). Each restrictor is located in the middle of each side of a grooved rectangular supply line with a base of 45 mm (a) and a width of 20 mm (b). The grooves present a triangular cross-section with a base of 0.2 mm (w_g) and a height of 0.06 mm (h_g).

Numerical Model

The system is modelled through lumped pneumatic resistances and capacitances (see Figure 2).

Materials Research Proceedings **26** (2023) 195-200 https://doi.org/10.21741/9781644902431-32

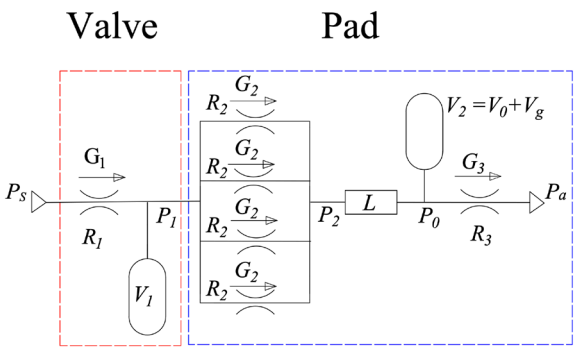

Figure 2: Pneumatic scheme of the prototype.

Starting from the upstream, the volume of the valve V_1 is supplied with a constant pressure P_s through the nozzle. The value of the air mass flow rate G_1 supplied by the nozzle (R1) depends on the initial position of the nozzle and its diameter d_n, the deflection of the membrane[1] x and its stiffness k_m, the supply pressure P_s and the pressure inside the valve chamber P_1. The air mass flow rate passing through the nozzle of the valve G_1 and the supply holes of the pad G_2 are computed by means of the ISO formula 6358 [16] as follows:

$$G_i = C_i P_s \sqrt{1 - \left(\frac{\frac{P_{d,i}}{P_{up,i}} - 0.5283}{1 - 0.5283} \right)^2} \qquad i = 1, 2.$$

$$C_1 = 1.05(1 - 0.3\, e^{-0.005\, Re_1}) \frac{0.685}{\sqrt{R\,T}}\, \pi\, d_n\, x; \qquad Re_1 = \frac{G_1}{\pi \mu d_n}$$

$$\begin{cases} x = 12\ \mu m; & x \le 12\ \mu m \\ x = x_n + \dfrac{\pi\, {d_m}^2}{4} \dfrac{(P_1 - P_a)}{k_m}; & x > 12 \mu m \end{cases} \tag{1}$$

$$C_2 = 1.05(1 - 0.3\, e^{-0.005\, Re_2}) \frac{0.685}{\sqrt{R\,T}} \left(\pi\, d_p\, h + w_g\, h_g\right)$$

$$Re_2 = \frac{G_2\, h}{\mu\left(\pi d_p h + w_g\ h_g\right)}$$

where, P_{up} and P_d are the upstream and downstream pressure. C_1 and C_2 are the pneumatic conductance related to the valve nozzle and the pad supply holes. G_3 is the mass flow rate exhausted through the air gap (R3) and it computed through Equation 2, where, P_0 is the mean constant pressure inside the area of the grooved rectangular supply line that is obtained from the pressure downstream the supply holes of the pad P_2 through the semi-empirical formula of Equation 3 [8] (that in Figure 2 corresponds to the function L) [14]. R, T and μ are the gas constant temperature and dynamic viscosity of the air. Re_1 and Re_2 are the Reynolds numbers related to the air flow passing through the nozzle of the valve and the supply holes of the pad.

[1] That is a function of the membrane geometry: its diameter d_m .

Materials Research Proceedings **26** (2023) 195-200 https://doi.org/10.21741/9781644902431-32

$$G_3 = \frac{1}{6\mu RT}\left(\frac{b}{A-a}+\frac{a}{B-b}\right)(P_0^2 - P_a^2)h^3 \tag{2}$$

$$P_0 = \left[1 - 0.14^{\left(\frac{5}{h}\right)}\right](P_2 - P_a) + P_a \tag{3}$$

The load carrying capacity of the pad F_p is computed through Equation 4 by assuming that the surface of the pad is perfectly smooth and that the pressure distribution outside the rectangular area surrounded by the grooves is linear.

$$F_p = \left[ab + AB + \frac{(Ab + aB)}{2}\right]\frac{(P_0 - P_a)}{3} \tag{4}$$

The dynamic equations of the model (Equations 5) that are necessary to compute the pressures (P_1 and P_0) along with the air gap height of the pad (h) are the continuity equations applied to volumes V_1 and V_0 and the equilibrium equation of the pad respectively:

$$G_1 - 4G_2 = \frac{V_1}{RT}\frac{dP_1}{dt} \qquad 4G_2 - G_3 = \frac{1}{RT}\left(P_0\frac{dV_2}{dt} + V_2\frac{dP_0}{dt}\right)$$
$$F^{ext} = F_p - M\ddot{h} \tag{5}$$

These equations are discretized by the Euler explicit method.

Numerical and Experimental Results

As it can be seen from Figures 3 the numerical model was experimentally validated through static characterizations. Moreover, the equations of the lumped model were exploited to implement a numerical design procedure in order to define the valve parameters that optimize the system performance around a specific air gap height h_{des}. To verify the accuracy and reliability of the proposed design procedure, it was used to compute the optimal operating parameters of the valve for an air gap height of 21 µm.

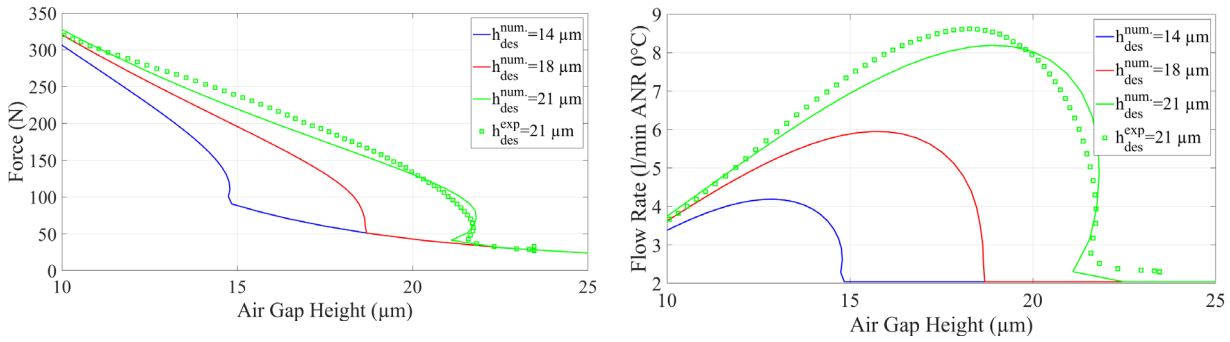

(a) Load Capacity (b) Air consumption

Figure 3: Experimental and numerical static feature of the prototype.

Figures 3 also reports the numerical curves that corresponds to operating air gap height $\boldsymbol{h_{des}}$ of 14 and 18 μm. Eventually, the stability of the prototype was experimentally verified around the operating air gap value (h_{des}=21 μm) through the application of a negative step force of about 20 N (see Figure 4).

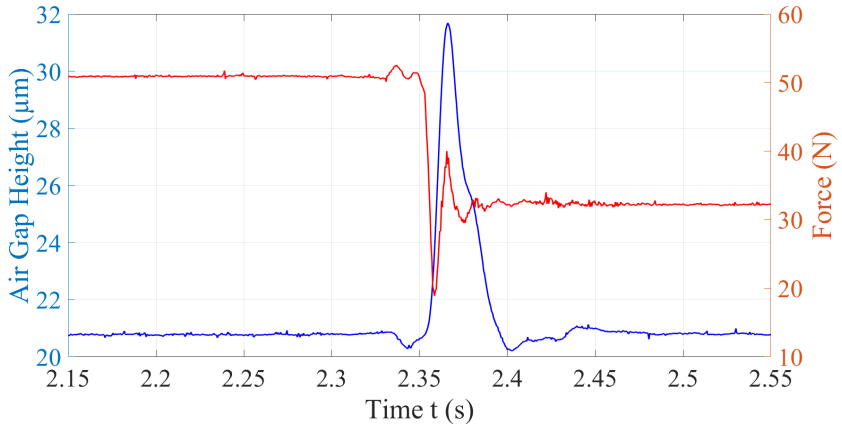

Figure 5: Step force test results (h_{des}=21 μm)

Step force test demonstrates the stability of the proposed prototype and even quasi-static infinite stiffness around the considered operating air gap height (h_{des}= 21 μm).

Conclusions

This paper presented a novel prototype of a passively compensated aerostatic pad consisting in the integration of a commercial pad and custom-built diaphragm valve. Compared to a previous solution, the new valve design was thought to obtain a simpler mechanical structure and higher repeatability. The repeatability was assessed by the fact that, conversely to the previous prototype, the initial position of the nozzle does not change after many experimental test repetitions. Moreover, the novel valve prototypes was built by exploiting a design algorithm (similar to those presented in [15]) based on the equation of the lumped parameter model of the system [14]. The static characterization of the prototype makes it possible to verify the accuracy of the lumped model and the proposed design algorithm. Step force tests were used to verify the stability of the system. Other than verifying the stability, step force tests demonstrated that the system is characterized by quasi-static infinite stiffness around the considered operating air gap height.

References

[1] Lentini L, Moradi M, Colombo F. A Historical Review of Gas Lubrication: From Reynolds to Active Compensations. Tribology in Industry 2018;40:165–82. https://doi.org/10.24874/ti.2018.40.02.01

[2] Gao Q, Chen W, Lu L, Huo D, Cheng K. Aerostatic bearings design and analysis with the application to precision engineering: State-of-the-art and future perspectives. Tribology International 2019;135:1–17. https://doi.org/10.1016/j.triboint.2019.02.020

[3] Colombo F, Lentini L, Raparelli T, Trivella A, Viktorov V. Dynamic Characterisation of Rectangular Aerostatic Pads with Multiple Inherent Orifices. Tribology Letters 2018;66. https://doi.org/10.1007/s11249-018-1087-x

[4] Luong TS, Potze W, Post JB, Van Ostayen RAJ, Van Beek A. Numerical and experimental analysis of aerostatic thrust bearings with porous restrictors. Tribology International 2004;37:825–32. https://doi.org/10.1016/j.triboint.2004.05.004

[5] Witelski T, Schwendeman D, Evans P. Analysis of Pressurized Porous Air Bearings. New Way Precision Air Bearings Inc; 2008.

[6] Colombo F, Lentini L, Raparelli T, Trivella A, Viktorov V. A Lumped Model for Grooved Aerostatic Pad. Advances in Service and Industrial Robotics, vol. 67, Springer International Publishing; 2019, p. 678–86. https://doi.org/10.1007/978-3-030-00232-9_71

[7] Colombo F, Lentini L, Raparelli T, Trivella A, Viktorov V. Dynamic model of a grooved thrust bearing: Numerical model and experimental validation. Proceeding of the 23rd Conference of the Italian Association of Theoretical and Applied Mechanics, AIMETA, vol. 4, 2017, p. 506–17.

[8] Colombo F, Lentini L, Raparelli T, Trivella A, Viktorov V. A nonlinear lumped parameter model of an externally pressurized rectangular grooved air pad bearing. Advances in Italian Mechanism Science, vol. 68, Springer; 2019, p. 490–7. https://doi.org/10.1007/978-3-030-03320-0_54

[9] Al-Bender F. Air Bearings: Theory, Design and Applications. John Wiley & Sons; 2021.

[10] Al-Bender F. On the modelling of the dynamic characteristics of aerostatic bearing films: From stability analysis to active compensation. Precision Engineering 2009;33:117–26. http://dx.doi.org/10.1016/j.precisioneng.2008.06.003

[11] Aguirre G, Al-Bender F, Van Brussel H. A multiphysics model for optimizing the design of active aerostatic thrust bearings. Precision Engineering 2010;34:507–15. https://doi.org/10.1016/j.precisioneng.2010.01.004

[12] Morosi S, Santos IF. Active lubrication applied to radial gas journal bearings. Part 1: Modeling. Tribology International 2011;44:1949–58. http://dx.doi.org/10.1016/j.triboint.2011.08.007

[13] Morosi S, Santos IF. On the modelling of hybrid aerostatic-gas journal bearings. Proceedings of the Institution of Mechanical Engineers, Part J: Journal of Engineering Tribology 2011;225:641–53. https://doi.org/10.1177/1350650111399845

[14] Ghodsiyeh D, Colombo F, Lentini L, Raparelli T, Trivella A, Viktorov V. An infinite stiffness aerostatic pad with a diaphragm valve. Tribology International 2020;141:105964. https://doi.org/10.1016/j.triboint.2019.105964

[15] Colombo F, Lentini L, Raparelli T, Trivella A, Viktorov V. Design and Analysis of an Aerostatic Pad Controlled by a Diaphragm Valve. Lubricants 2021;9:47. https://doi.org/10.3390/lubricants9050047

[16] Belforte G, Raparelli T, Viktorov V, Trivella A. Discharge coefficients of orifice-type restrictor for aerostatic bearings. Tribology International 2007;40:512–21. https://doi.org/10.1016/j.triboint.2006.05.003